1-1-2002

Anodic Behavior of Ti in KOH Solutions: Ellipsometric and Micro-Raman Spectroscopy Studies

A. Prusi
University Kiril and Metodij, Skopje, Macedonia

Lj. Arsov
University Kiril and Metodij, Skopje, Macedonia

Bala Haran
University of South Carolina - Columbia

Branko N. Popov
University of South Carolina - Columbia, popov@engr.sc.edu

Publication Info

Journal of the Electrochemical Society, 2002, pages B491-B498.

Publisher's link: http://dx.doi.org/10.1149/1.1510134
DOI: 10.1149/1.1510134

Journal of The Electrochemical Society, **149** (11) B491-B498 (2002)
0013-4651/2002/149(11)/B491/8/$7.00 © The Electrochemical Society, Inc.

Anodic Behavior of Ti in KOH Solutions

Ellipsometric and Micro-Raman Spectroscopy Studies

A. Prusi,[a] Lj. Arsov,[a] Bala Haran,[b,*] and Branko N. Popov[b,*,z]

[a]*Faculty of Technology and Metallurgy, University Kiril and Metodij, Skopje 91000, Macedonia*
[b]*Department of Chemical Engineering, University of South Carolina, Columbia, South Carolina 29208, USA*

Anodic formation of oxide films on titanium surfaces, in various concentrations of aqueous KOH solutions, have been studied using ellipsometry and micro-Raman spectroscopy. By *in situ* ellipsometric measurements the coefficient of film thickness growth and indexes of refraction of anodic oxide films have been determined. The voltage at which the oxide film breaks down is strongly dependent on the KOH concentration. Further, the solution concentration strongly influences the potential at which the oxide film is transformed from the amorphous state to crystalline form. Using micro-Raman spectroscopy four crystalline forms of titanium oxides, namely, anatase, brookite, corundum, and rutile, have been identified. The crystalline form of the surface oxide is shown to depend on the applied voltage and on the time of anodization. The micro-Raman spectra reveal that brookite and corundum are intermediate forms of the anodic oxide films and the final film formed is primarly composed of an anatase type of TiO_2.
 [DOI: 10.1149/1.1510134]

Manuscript submitted January 14, 2002; revised manuscript received April 15, 2002. Available electronically September 18, 2002.

Over the last three decades, there has been a growing interest for the use of titanium and its alloys in various branches of chemical industry, specifically in transport and stocking of aggressive fluids, electrosynthesis, photoelectrochemical activity, and solar energy conversion. The use of Ti in such wide range of applications arises due to its excellent corrosion resistance. Ti instantaneously forms a surface oxide film when exposed to the atmosphere. The excellent corrosion resistance of Ti is attributed to this spontaneous natural surface oxide film. While the film is highly resistive and is extremely stable to a wide range of contaminants, it has been shown that the natural oxide film dissolves slowly in dilute acid and alkaline solutions. The decrease in corrosion resistivity after exposure to dilute acid solutions has been attributed to the uniform dissolution of the surface oxide.[1] However, the stability of the metal in such environments can be easily restored by anodic oxidation. This attribute of Ti favors it as the material of choice for use in highly corrosive environments. Through anodic oxidation and formation of passive films, it is easily possible to prevent rapid dissolution of the underlying metal and continuously replenish the surface oxide. Further, this method is highly attractive since Ti possesses a wide potential window during which the metal remains in the passive range. Also, the large range of the passivation potentials are observed in most environments.

Anodic oxidation is a well-established procedure in the case of many metals, but in the case of titanium in strong alkaline solutions, relatively little conclusive information is available, and procedures are not well developed. In most cases, films prepared are semiconducting in nature and are nonstoichiometric in composition.

It should be noted that many references to the anodization of titanium, in a variety of acid and salt-type electrolytes, exist in the literature.[2-5] The growth of anodic oxide films has been extensively studied and is well established, particularly in the case of sulfuric, hydrochloric, and phosphoric acids.[6-8] In general, acid electrolytes gave by far the best results and the most homogeneous films. However, very strong acids, such as HF, HNO_3, and $HClO_4$ have a strong tendency toward dissolving the films produced. Hence, oxide films formed in these solutions have a tendency to retain a highly porous structure, especially at higher potential of anodization, and thus, the electrical properties are somewhat undesirable. Oxidation in very weak acids, such as organic acids, produces homogeneity, but limits the thickness of the translucent films. The phosphate-based acids and salts, from our knowledge, gave by far the best results. The advantage with these electrolytes was the ease with which it was possible to build anodic films at high potentials. Further, the oxide films had a low porosity and excellent corrosion resistance. In the evolution of superior anodic films, a wide range of film parameters need to be studied, namely, oxide thickness, homogeneity, density, porosity, and electrical properties.

So far relatively less attention has been paid to the anodization and passivity behavior of titanium in alkaline solutions. Specifically not much attention has been paid to anodization in high-alkali solutions. Not much literature data can be found concerning the electrochemical polarization of Ti in alkaline solutions, where many processes related to chemical and electrochemical film formation, as well as destruction of oxide films, occur. Further, among the existing data there exists a divergence of results and large disagreement regarding the explanation for the mechanism of different reactions, mainly due to the formation of numerous metastable and intermediary products adsorbed on the Ti surface.[9-11] Strong alkaline electrolytes either resulted in precipitates of titanium oxide or reacted so rapidly with the titanium surface that the entire substrate was quickly converted to oxide.[11] Thus, it was difficult to control the anodic process utilizing strong alkaline electrolytes. Evidently, each process that occurs on the Ti surface during electrochemical polarization is actually driven by the cumulative effects of complex spontaneous and initialized electrochemical reactions. These two processes can be examined separately only at open-circuit potential, where there are no net current electrochemical processes, or at high anodic potentials, when the rate of the spontaneous processes is negligible as compared to that of the electrochemically initialized ones.

In our previous papers we have studied very systematically the growth kinetics of spontaneously formed films on titanium surfaces, under open-circuit conditions, in various concentrations of potassium hydroxide solutions.[10] Since our previous research yielded a fair knowledge of the different chemical reactions and processes which cause oxide buildup at open circuit, in this paper we extend this methodology to determine the microstructure and film thickness growth of anodically formed films on Ti surfaces in strong KOH solutions. The film growth has been studied as a function of applied potential and potassium hydroxide concentration. Ellipsometry and micro-Raman spectroscopy proved to be useful techniques in revealing surface processes. The film thickness and optical properties of the films were studied by ellipsometry, while its microstructure was studied using micro-Raman spectroscopy. Furthermore, the film breakdown is discussed on the basis of anodic voltage, electrolyte concentration, film thickness, and micro-Raman observations on particular grains of the film.

Experimental

Electrodes.—The working electrode was constructed from a 25 mm diam commercial pure 99.7% Ti rod (U.T.40 Ugine Kuhleman).

* Electrochemical Society Active Member.
z E-mail: popov@engr.sc.edu

Ti rods were cut from an annealed sheet in the form of cylinders with height of 10 mm. Subsequently, each cylinder was embedded in epoxy resin (Struers) leaving one end to be in contact with solution in the electrolytic cell. In this arrangement, the titanium electrodes with a surface area of 4.9 cm^2 were mechanically polished using emery paper 600. After this rough polishing, they were degreased and ultrasonically cleaned with methanol and finally electropolished to a mirror brightness according to the procedure suggested in Ref. 12. For checking the quality of electropolishing, before anodization each sample was tested ellipsometrically. After completion of the experiment an extensive mechanical repolishing was necessary in order to avoid any traces of film formation from the previous experiment. A Pt grid with large surface area was used as a counter electrode, and saturated calomel electrode (SCE) served as the reference.

Optical electrolytic cell.—A three-compartment optical-electrolytic cell was adopted for electrochmical-ellipsometric *in situ* measurements. Experiments were done in a Pyrex vessel 250 cm^3 in capacity with two optical quartz windows fixed at an angle of incidence of 70° and similar in design to those described in Ref. 13. A. Luggin probe reference electrode assembly, containing an isolating stopcock to avoid contamination from the reference electrode by the chloride solution, was employed. Prior to running any experiments, the solution in the cell was deaerated by flowing argon gas through a fritted bubbler for at least 30 min. The gas flow was discontinued during the run.

Solutions.—Aqueous solutions (Acros Organics), p.a. with concentrations of: 0.1, 1, and 5 M KOH were prepared in redistilled and deionized water. The electrolyte was exchanged after each measurement in order to avoid buildup of soluble Ti species that are known to enhance the stability of the surface oxides.

Apparatus.—The anodic oxidation from 0 to 10 V (*vs.* SCE) was performed potentiostatically using a Heka model 488 potentiostat/galvanostat interfaced with a personal computer and connected to a Philips X-2Y recorder, model PM 8272. The potential was increased in increments of 0.5 V SCE and polarization studies were done in the range between 0 and 10 V SCE. For voltages higher than 10 V SCE, the same potentiostat/galvanostat was utilized but as a two-electrode system. In this case, the voltage was increased every 2.5 V up to 90 V. For voltages greater than 90 V, a highly stabilized two-electrode voltage supply ''Drusch 5140'' was utilized. The ellipsometric measurements were performed with a Rudolph Research type 43603-200 thin-film ellipsometer at a wavelength of 546.1 nm and an incident angle of 70°.

The micro-Raman spectra were recorded using an Omars Microdil 28 equipped with argon ion laser operating with 1 mW power at the sample for excitation of 514.5 nm.

Results

At open-circuit potential, as soon as the Ti electrode is immersed in alkaline solution, the process of dissolution of natural oxide film begins simultaneously with self-passivated film formation. By ellipsometric measurements, we have shown in our previous paper that the spontaneous formation and growth of the oxide film follows several steps, which depend on time and concentration of KOH solutions.[10] During the film growth, film dissolution also occurrs and it was surprising that the rate of film dissolution was higher in strong alkaline solutions than in strong acid solutions. This was the main reason why the films formed in strong alkaline solutions, for a given anodic voltage, were more inhomogeneous than those formed in strong acid solutions.

After the natural oxide film dissolves partly or completely, the self-formed films in the beginning consist mostly of $Ti(OH)_3$, which is in accordance with Pourbaix diagrams.[14] As film thickness increases, $Ti(OH)_3$ converts to the hydrated oxide $TiO_2 \cdot 2H_2O$, and dynamic equilibrium between these two different types of films is established as follows

$$Ti(OH)_3 \leftrightarrows TiO_2 \cdot H_2O + 1/2H_2$$

This equilibrium depends only upon the physical properties of the solution (concentration and temperature), *i.e.*, it is closely related with the number of bonding OH^- ions. The anodic oxidation perturbs the equilibrium as given by Eq. 1, and the film growth is controlled mainly by applied potential. This begins after 30 s of polarization and increases with time of anodization.

Ellipsometry.—Ellipsometry, is one of the most convenient and accurate techniques for the measurements of film thickness and refractive indexes of thin films on solid surfaces. The characterization of a thin film grown on a metallic substrate requires a preliminary knowledge of the optical indexes of the substrate and surrounding media. However, the principal difficulty is that a superficial natural oxide film is always present on the metallic surface. Thus, the optical indexes of both the metal and its natural oxide film must be measured together. The refractive indexes determined for the titanium metal substrate were found to depend on the preparation procedure adopted for the electrode and on the prepolarization time.[15]

The refractive index of the oxide-free Ti surface has been established in our previous paper through ellipsometric measurements of a cathodically polarized Ti surface at −0.6 V SCE in 0.5 M H_2SO_4.[13] At this potential the electrochemical reduction of natural oxide film occurred across the electrode surface, without formation of hydrated layers, but it seems unlikely that an completely oxide- or hydride-free Ti surface can be prepared under electrochemical conditions. Our computed values of the complex refractive index of free-oxide metal surface are $\hat{n}_3 = 2.94(1\text{-}1.217.i)$. These values are very close to the data reported in literature for Ti prepared by evaporation in vacuum and measured in high vacuum.[16]

For anodic oxide films, formed in various concentrations of KOH solutions, the ellipsometric *in situ* measurements were performed in the potential region between the steady-state potential at open circuit and a set anodic potential. The upper limit of the anodic potential was set at the point at which intensive oxygen evolution on Ti electrode occurs, accompanied by current oscillations and film breakdown. The current oscillations are related to a sparking phenomenon, which could sometimes be observed visually on the electrode surface. Usually the sparking phenomena can be monitored indirectly by the onset of small oscillations in the current. The breakdown voltage was defined as the voltage at which the invisible sparking was observed to start with small current oscillations. In order to record precisely the first oscillations of the cell current, an oscilloscope was inserted between the electrodes. The upper limit of the anodic potential at which isolated sparks are observed depends strongly on the KOH concentrations. At low KOH concentrations the breakdown of the film occurs uniformly across the Ti surface, while at large KOH concentrations, the breakdown could involve local attack, leading to the formation of big pores. It should be mentioned that at the onset of the upper limit to the anodic potential small invisible sparks initially randomly spread on the electrode surface. Above this limit, the sparks gather gradually and finally form a visible electrical arc moving freely on the electrode surface. This suggests that sparking may be the electrical discharge through gas generated at the anode surface and is associated with a strong field that extends into the solution. In our measurements sparking voltage is defined as the potential at which sparking begins over the entire sample surface and is accompanied by rapid current fluctuations.

The relevant parameters governing the anodic oxidation are given in Table I. In order to ensure accurate ellipsometric measurements, for each concentration of KOH, when the working electrode was polarized to potentials more than 2 V *vs.* SCE, after 30 s of polarization the potential was rapidly diminished and brought back to the constant value of 2 V *vs.* SCE. For the two-electrode system the potentiostat was programmable and after 30 s of polarization it automatically diminished the potential to 2 V SCE. For higher voltages than 90 V, the electrode was connected to both a high-voltage

Table I. Breakdown voltage, spark voltage, and refractive indexes of Ti electrode as a function of KOH content.

Concentration of KOH (M)	Limit anodic voltage Breakdown voltage (V)	Visible spark Spark voltage (V)	Refractive index
0.1	>100	>100	$\hat{n}_2 = 2.42(1\text{-}0.006.i)$
1.0	70	72	$\hat{n}_2 = 2.39(1\text{-}0.009.i)$
5.0	6	8	-

supply and a potentiostat. The electrode voltage was maintained through the power supply. When after 30 s of anodization the high-voltage supply was switched off the potentiostat was automatically switched on by a special relay and set at a potential of 2 V *vs.* SCE. This was done for each applied perturbation and was primarily to prevent oxygen bubbles from accumulating at the surface. This helped in avoiding the incident elliptically polarized beam from interference during evolution of gas bubbles on the electrode surface at large anodic voltages.

It is well known that in ellipsometric measurements the experimentally measured parameters Δ and ψ are related to the physical properties of the system by the use of Fresnel's equation, which permits the calculation of the reflective index of a reflecting surface.[17] For a three-component system (medium, oxide film, metal substrate) the experimentally measured ellispometric parameters Δ and ψ would be related as a complex function as given here

$$tg\psi \exp(i\Delta) = \frac{r_{1,2,p} + r_{2,3,p}\exp(-2i\delta)}{1 + r_{1,2,p}r_{2,3,p}\exp(-2i\delta)} \frac{1 + r_{1,2,s}r_{2,3,s}\exp(-2i\delta)}{r_{1,2,s} + r_{2,3,s}\exp(-2i\delta)} \quad [1]$$

In Eq. 1 $tg\psi$ represents relative amplitude attenuation, Δ is relative phase change, r_p and r_s represent the Fresnel reflections coefficients for light polarized parallel and perpendicular to the plane of incidence, respectively, while the subscripts 1, 2, and 3 correspond to medium, film, and metal substrate, respectively. In mathematical expressions of the Fresnel reflection coefficients the values of complex refractive indexes $\hat{n}_1 = n_1(1 - ik_1)$, $\hat{n}_2 = n_2(1 - ik_2)$, and $\hat{n}_3 = n_3(1 - ik_3)$ correspond to medium, film, and metal substrate, respectively. The values of n_1, n_2, and n_3 represent refractive indexes (real parts), while the values of k_1, k_2, and k_3 represent extinction indexes (imaginary parts). In Eq. 1 δ represents change of phase of the beam crossing the film and is given by

$$\delta = \frac{2\pi}{\lambda} d(\hat{n}_2^2 - \hat{n}_1^2 \sin in^2\varphi_1)^{1/2} \quad [2]$$

In Eq. 2 λ, φ_1, and d represent wavelength of incidence light, angle of incidence of the incident light, and thickness of the film, respectively.

In Eq. 1 and 2 the unknown parameters are $\hat{n}_2$ and d. The values of Δ and ψ are obtained from ellipsometric readings, and the value of φ_1 and λ are given by us. The refractive index $\hat{n}_1$ of the medium can be determined by Abbe's refractometer, while the index of refraction of metal substrate $\hat{n}_3$ is known from our previous investigations, which was also ellipsometrically.[13] The refractive index of the anodic oxide films $\hat{n}_2$ and the film thickness d can be simply determined by fitting the experimentally measured parameters Δ and ψ with theoretical Δ-ψ curves, which are computed for fixed values of $\hat{n}_1$ and $\hat{n}_3$ utilizing Eq. 1.

The fitting procedure was performed according to the mathematical method and equations given in Ref. 18. During the fitting procedure the value of $\hat{n}_2$ was searched for prior given values of d, from our side, in increasing direction. The correct value for the searched parameters $\hat{n}_2$ and d can only be obtained if the number of theoretical points is at least ten times more than the number of experimental ones.

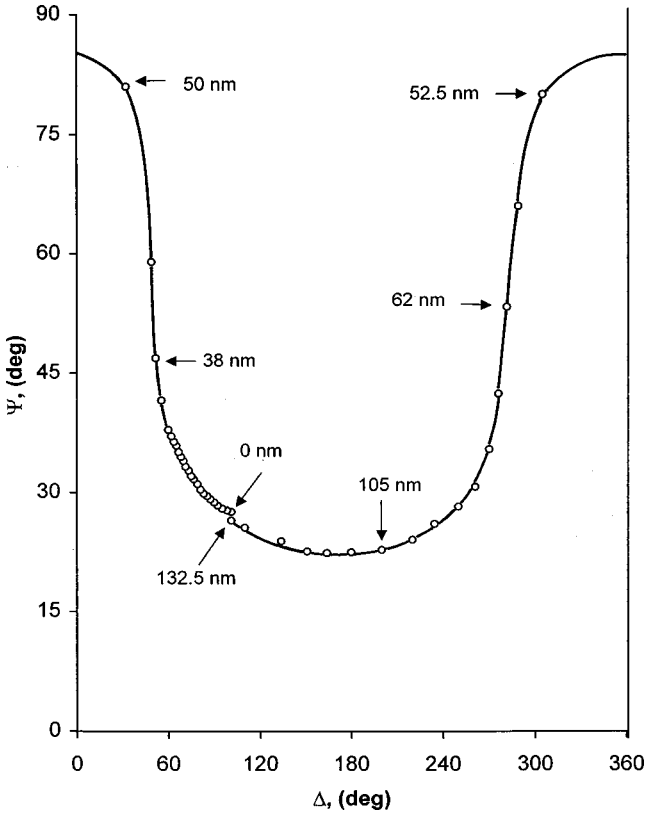

Figure 1. Graphical presentation of experimentally measured Δ and ψ (○) during the anodic oxidation of Ti in 0.1 M KOH for various values of applied voltages. (——) The computed fitting curve given by Eq. 1. The fitted value for film refractive indexes are $\hat{n}_2 = 2.42(1\text{-}0.006.i)$. On the computed curve some values of film thickness are shown.

In order to determine the kinetic law for film thickness growth on Ti surface, the ellipsometric measurements were performed in three different concentrations of KOH, 0.1, 1, and 5 M, and for various applied anodic potentials.

In Fig. 1 the experimentally measured Δ-ψ parameters for anodically formed films in 0.1 M KOH are fitted to the theoretically computed Δ-ψ curve. Each experimental Δ-Ψ point on Fig. 1 corresponds to the exact applied potential or voltage of anodization. On some points in Fig. 1 the values of film thickness are added. For the theoretical Δ-ψ fitting curve the fixed values are $\hat{n}_1 = 1.3345(1\text{-}0.i)$ for 0.1 M KOH (as determined by Abbe's refractometer) and $\hat{n}_3 = 2.94(1\text{-}1.217.i)$ for Ti substrate, while the searched value of $\hat{n}_2 = 2.42(1\text{-}0.006.i)$ was found. The searched value of $\hat{n}_2$ for all investigated concentrations of KOH are also given in Table I. The number of theoretical Δ-ψ points on the computed curve depends on the thickness increments, given during the computation. For small values of thickness increments the computed curve has a large number of theoretical Δ-ψ points and the film thickness during the anodization can be determined more precisely. On Fig. 1 for computation we have utilized 135 theoretical points with thickness increment of 1 nm, and this is the main reason why the theoretical curve has a continuous shape.

From the experimentally measured Δ-ψ plot in Fig. 1 the voltage difference of 56 V between 0 (beginning of the anodization) and 56 V (terminus of the first lap) is determined. The theoretical curve (line) represents the locus of the Δ-ψ points with increasing thickness. The arrows show the direction of increasing thickness. From

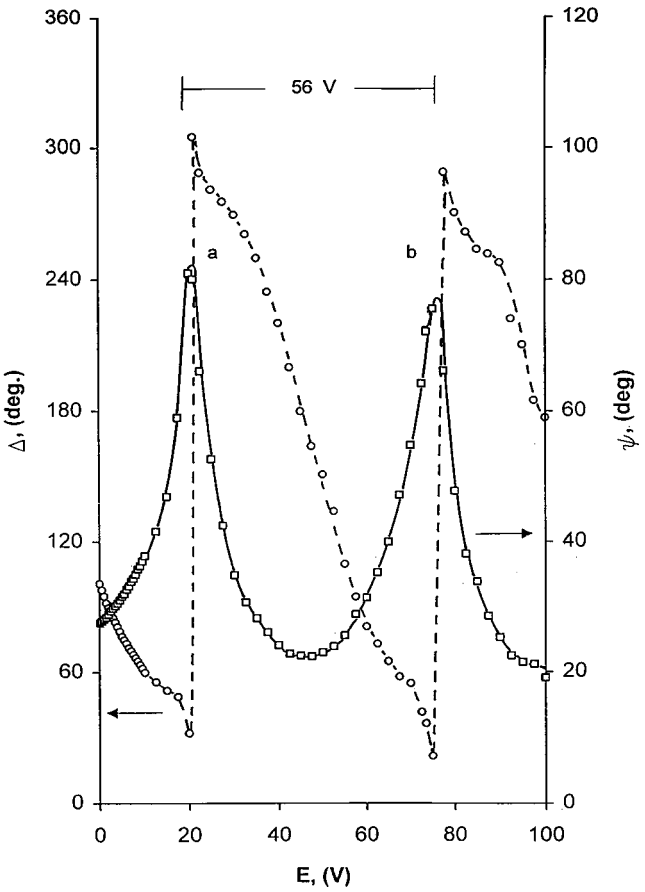

Figure 2. Graphical presentation of experimentally measured (○) Δ and (□) ψ in 0.1 M KOH as a function of anodic voltage. (— — —, ——) Theoretical fitted curves by Eq. 1 for Δ and ψ, respectively.

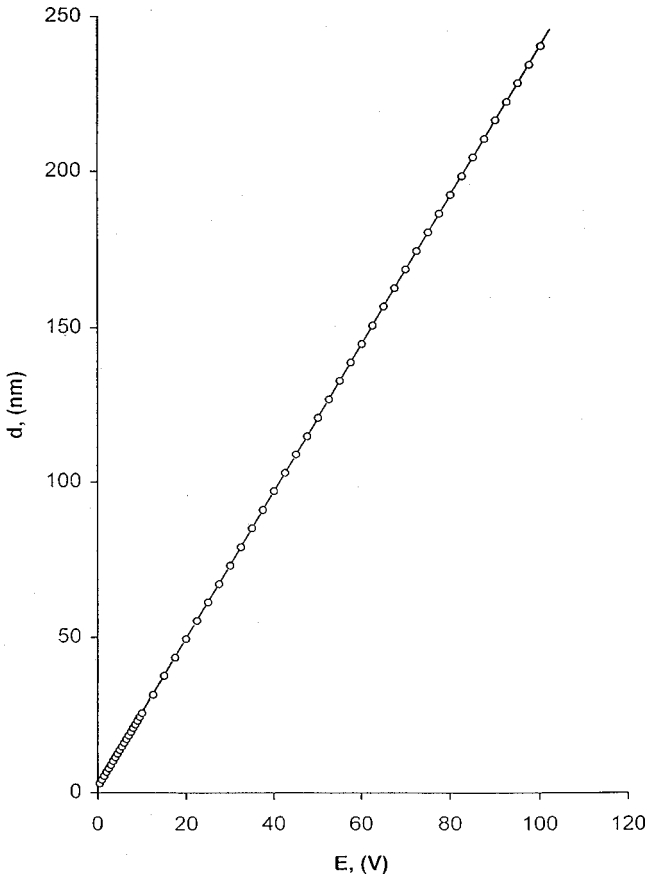

Figure 3. Dependence of film thickness grown from anodic voltage on Ti surface in 0.1 M KOH.

the theoretical computed curve the value of 56 V corresponds to a film thickness of $d = 132.5$ nm. For anodization voltages higher than 56 V and films thicker than 132.5 nm the experimentally measured Δ-ψ and theoretically computed curve begin their second cycle but they do not end at the same point where they started. The second cycle does not overlap the first one and Δ and ψ do not have a cyclic dependence on thickness. In contrast, for transparent nonabsorbing isotropic film ($k_2 = 0$) the plot of the Δ-ψ curve is a cyclic function of film thickness and repeats periodically with every 180° change in δ.[18]

On Fig. 2, the variation of experimentally measured Δ and ψ and theoretically computed Δ and ψ curves with applied voltage are shown. The curve for Δ has two large drops (a) and (b) which correspond to the sharp and well-defined peaks on the curve for ψ. From the distance between the peaks (a) and (b) on the curve for ψ, *i.e.*, points of inflection of two large drops on the curve for Δ, we can determine the film thickness. In this case, the difference in voltage is 56 V for a change in value of Δ of 360°. This voltage difference corresponds to a film thickness of 132.5 nm as determined by theoretical fitting the curve on Fig. 1. As shown in Fig. 1 and 2 there is fairly good agreement between the experimental loci and the theoretical fitted curve in the investigated voltage range. Since the same values for the voltage difference, 56 V, and film thickness growth, 132.5 nm, are seen in various voltage regions (0-56 V Fig. 1 and 20.5-76.5 V Fig. 2), it is evident that the film thickness growth must be a linear function of potential in the investigated voltage region. Moreover, for anodization voltage of 20.5 and 76.5 V on titanium surfaces, the films with the same interferential color (blue) are formed. This is quite reasonable because for this voltage difference the change in Δ is 360° and in $\delta = 180°$. The curves for Δ and Ψ were derived from Fig. 1 and the position of peaks (a) and (b) correspond to the theoretical fitting curve on Fig. 1 for $\Delta = 0$ in the first cycle and for $\Delta = 0$ in the second cycle. For clarity on Fig. 1 the values of Δ and Ψ for voltages higher than 56 V in the second cycle are not shown. From values for the voltage difference of 56 V and corresponding thickness of 132.5 nm we can approximately calculate the coefficient of film thickness growth per volt, *i.e.*, $\alpha = 132.5/56 = 2.36$ nm/V. If k_2 was 0 and the Δ-ψ curve was a cyclic function of film thickness, the value of 2.36 nm/V should be the exact value, but in our case $k_2 = 0.006$ and the calculated approximate value of α is reasonable.

From Fig. 2, comparing the experimentally measured Δ and ψ values with theoretically fitted curves utilizing Eq. 1, the kinetic rate of film thickness growth and exact value of α were determined. These results are shown in Fig. 3. As can be seen from Fig. 3 in the measured voltage range the film thickness growth is a linear function of applied voltage and is given by the following relation

$$d = aV + b \qquad [3]$$

From the slope of the linear function on Fig. 3 the exact value of the coefficient *a* (2.38 nm/V) in 0.1 M KOH was determined. Data from studies at different concentrations and temperature reveal that the coefficient α depends strongly on these two parameters. This dependence is given in Table II. The coefficient *b* (1.86 nm) is the intercept of the straight line in Fig. 3 with the ordinate axis at a potential close to 0 V *vs.* SCE. The steady-state potentials of electropolished Ti surfaces in various concentrations of KOH always have more cathodic values than 0 V *vs.* SCE.[10] Hence, in this case at 0 V *vs.* SCE a small anodic current flows through the electrochemical cell.

Table II. Coefficient of film thickness growth on Ti surface as a function of KOH concentration and temperature.

Concentration of KOH (M)	Coefficient of film thickness growth (nm V^{-1})		
	0°C	20°C	40°C
0.1	2.12	2.38	2.47
1.0	2.26	2.42	2.51
5.0	2.93	3.47	3.72

This current could cause formation of a thin anodic film, which in 0.1 M KOH reaches the thickness of 1.86 nm after 30 s. For anodization at potentials greater than the anodic limit potential the rate of film growth follows a parabolic path as compared to the linear increase seen in Fig. 3. For each concentration given in Table II these shifts are caused by rapid augmentation of the film pores and the breakdown process. With time the oxide films become inhomogeneous, causing a number of structural defects. These defects can be observed by a metallographic microscope as a variety of different interference colors that exist between the grains of the film. The inhomogeneity of the film imposes limitations on the voltage range in which the ellipsometric measurements can be done. For 1 and 5 M KOH the film breakdown begins at lower potentials as compared to at 0.1 M KOH. Hence, in these cases the ellipsometric measurements were performed over a shorter range of applied anodic voltages than in 0.1 M KOH.

Figure 4 presents the variation of film thickness with time of anodization for different applied voltages. As seen on this figure at all applied voltages, most of the film growth occurs within the first 30 s. After 30 s the film growth for voltages of 50 and 75 V are small and for 20 V the growth is negligible. At an applied voltage of 50 V the film continues to grows from 30 s to 3 min, while at a voltage of 75 V the film grows slightly longer to 5 min. At 75 V, the film continues to grow even after 5 min, but with very small thickness increments.

Microscopic observations reveal that prolonged anodization beyond 30 s initializes intergranular corrosion which progresses with time. This progress is more rapid at higher voltages and the film becomes less homogeneous. For large voltages, the increase of thickness for prolonged anodization can be attributed to augmentation of the number of local microbreakdown centers on the electrode surface, where the conductivity is increased resulting in formation of new, thicker microlayers.

Micro-Raman spectroscopy.—Micro-Raman spectroscopy is a powerful tool for characterization of electrode surface layers and anodic oxide films on the substrate grains. For detection of crystal structure the Raman effect is a satisfactory alternative procedure to the standard X-ray and electron diffraction techniques. Raman spectroscopy offers the advantages of more simple sample preparation and rapidity of measurements. With conventional Raman spectroscopy the incident laser beam falls on about 2 mm^2 of the investigated sample. The Raman scattered light, which is monitored, represents an average value of all the grains that are illuminated with the incident laser beam, but in the case of titanium, the grains of anodically formed films have various colors and different crystallographic structure, as a result of breakdown, especially at large anodization voltages. With micro-Raman spectroscopy, the microlaser beam is centered by the microscopy device just on one grain and then its structure is examined. This procedure can be continued on each surface grain on the structure to obtain a complete picture on the microstructure of all grains on the examined metal surface.

The natural oxide film on electropolished Ti surfaces so far has been studied using various diffraction and spectroscopical techniques. By measurements of short-angle camera the X-ray diffraction (XRD) patterns have shown that the natural oxide film was TiO_2 with peaks for *d* lines, which correspond to rutile structure.[10] Hugot-Le Goff reported the existence of active Raman bands for

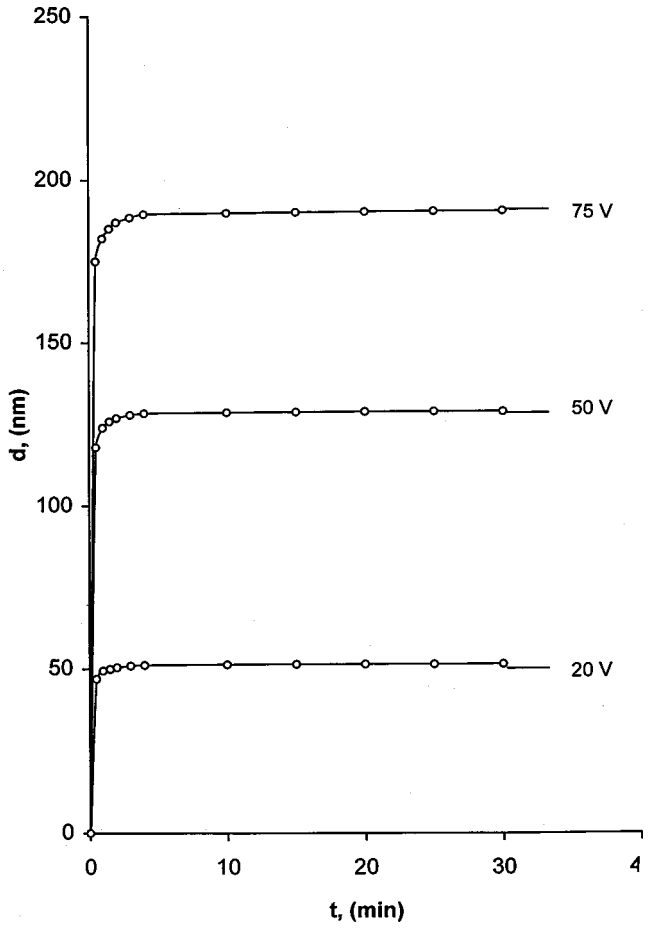

Figure 4. Dependence of film thickness on the time of anodization for various applied voltages on Ti surface in 0.1 M KOH.

very thin TiO_2 natural oxide films different than those of bulk rutile and anatase.[19] Recently, Birch and Burleigh presented existence of an amorphous oxide on an electropolished Ti surface with chemical composition of $TiO_2(H_2O)x$.[20] Our micro-Raman measurements of the freshly electropolished Ti surface have shown high disorder of the amorphous phase belonging to the natural oxide films. Further studies need to be done to establish the chemical composition, structure, and crystal modification of natural oxide film on Ti.

The appearance of active micro-Raman bands on anodized titanium surfaces was found to be a function of KOH concentration, applied voltage, and anodization time. When the anodization time is fixed at 30 s no active micro-Raman spectra were recorded in 0.1 M KOH until a voltage of 25 V was reached. After 30 s at this voltage only one weak band was observed at 144 cm^{-1} [see Fig. 5, spectrum (a)]. Oxidation for more than 30 s reveals supplemental bands at 400, 516, and 640 cm^{-1}, which belong to the anatase mineral form. With stepwise increase in the anodic voltage the micro-Raman bands develop in intensity, and at 100 V (the highest voltage employed in this work) five well-defined (one strong, three medium, and one weak) bands characteristic of the anatase mineral form were seen [see Fig. 5, spectrum (b)].

In 1 M KOH, the strongest micro-Raman band at 144 cm^{-1} becomes noticeable even at 15 V after anodizing for 30 min. At 50 V all characteristic micro-Raman bands for anatase mineral form are well developed and have similar shape as the spectrum given on Fig. 5b. At 70 V only anatase form of Ti oxide was seen. The anodic oxide film is generally uniform and most of the grains have pale green color. Only a few grains present red colors, and micro-Raman spectra of these grains showed also anatase structure but with a little

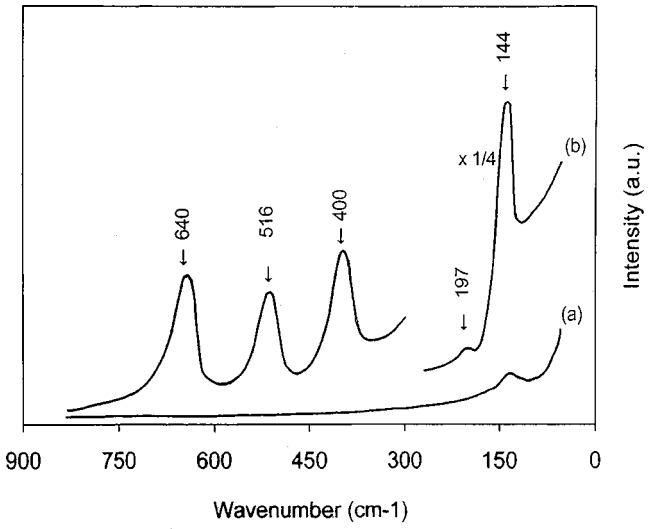

Figure 5. Micro-Raman spectra of Ti surface anodically oxidized for 30 s in 0.1 M KOH: (a) 25 and (b) 100 V.

bit lower intensity. Very fine dark spots are randomly dispersed on some green grains and it seems that these spots form clusters. At an anodic voltage of 72 V sudden current oscillations and visible sparks on the electrode surface were observed. For relatively short anodization time (about 10 s), as a result of local spark, some big craters are formed on the electrode surface as shown in Fig. 6. If the microlaser beam is centered just on the crater, sixteen bands, including two shoulders, were seen. Six of the observed bands and one shoulder can be assigned to the anatase [144 (s), 399 (m), 518 (m), and 643 (m) cm^{-1}] and rutile [236 (m), 452 (m), and 616 (sh) cm^{-1}] structures.[21] The other bands probably belong to one or more additional mineral form of titanium structure. According to literature data and measurements obtained with conventional Raman spectroscopy, the bands located at 205 (medium), 320 (weak), 363 (weak), and 412 (shoulder) cm^{-1} belong to TiO_2 (brookite) structure, while the strongest band located at 280 (strong) cm^{-1} is the key band of the substoichiometric Ti_2O_3 (corundum) mineral form.[22] The bands located at 751 (weak) and 860 (medium) cm^{-1} do not belong to any known mineral form of titanium oxides. If the microlaser beam is centered on any of the other grains around the crater, the strong spectrum of only anatase mineral form was recorded. For prolonged anodization on the same sample from 10 to 60 s, as a result of intensive spark, the electrode surface became covered with a white layer (like powder) of TiO_2 which is not adherent and peels off from the electrode surface. Micro-Raman spectrum of this layer gives well-defined peaks of only rutile structure as shown in Fig. 7.

Discussion

In literature data there exists a very big discrepancy about the coefficient of film thickness growth (2.0-2.6 nm V^{-1}) and values of complex index of refraction of the anodic films n_2 (2.00-2.53) and k_2 (0-0.318).[13,23-26] This discrepancy is mainly due to the different manners of surface preparation, the variety of anodization methods employed, and the use of various procedures for calculations, which sometimes provoke very significant errors. Comparing the results of previous studies with results in this work, it should be noticed that significant distortions resulting from electrolyte concentration appear to arise primarily due to the ability of the electrolyte to dissolve the resultant anodic film. In our previous work, by comparing electrochemical and ellipsometric measurements we have shown that the films grown on electropolished Ti surfaces are more resistant and do not break down as readily as films grown on mechanically polished and etched Ti surfaces.[13,15,18]

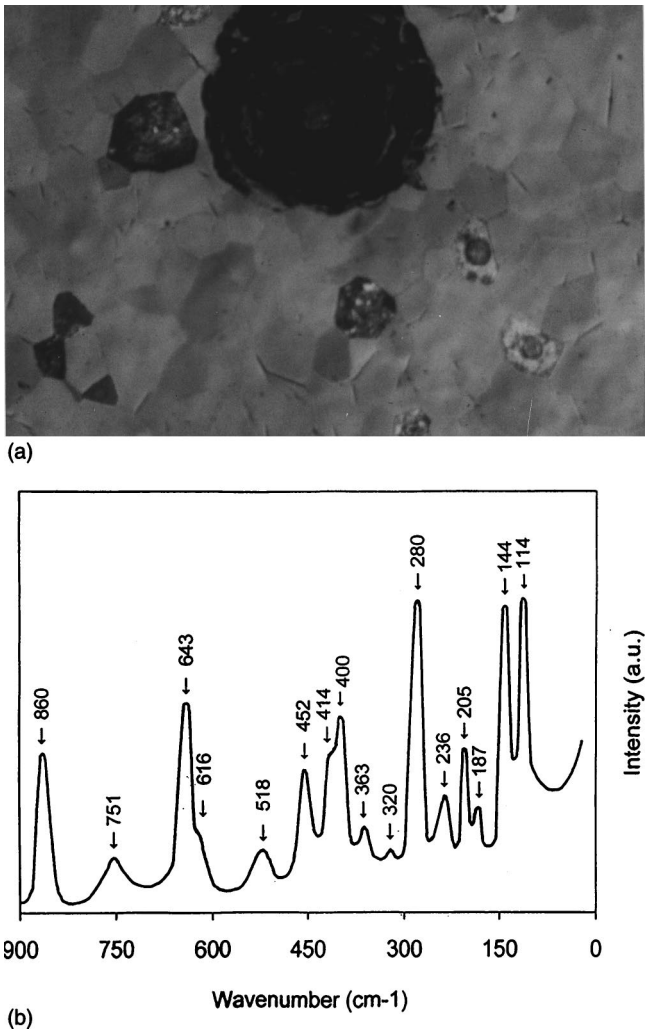

Figure 6. Metallographic photo (a) of Ti surface anodically oxidized for 10 s at 72 V in 1 M KOH and (b) micro-Raman spectrum of crater.

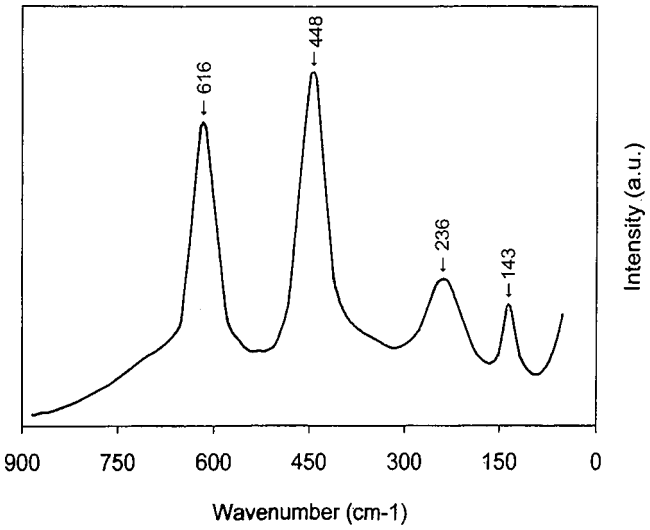

Figure 7. Micro-Raman spectrum of Ti surface anodically oxidized for 60 s at 72 V in 1 M KOH.

Electrolytes possessing no solvent action produce relatively thin films with poor electrical characteristics. Electrolytes possessing extreme solvent action characteristics yield poorly adherent and inhomogeneous films, especially those formed at higher anodic voltages. In these electrolytes, there are no significant effects. For these electrolytes, as in our case for KOH, the resulting effects of electrolyte concentration changes on the film thickness growth and on the refractive indexes of the formed films are significant. The coefficient of film thickness growth increases much more in higher concentration of KOH than in lower. Similar effects are also seen as a function of temperature as seen in Table II. The anodic film thickness increases with increase in KOH concentration, probably due to the bigger influence of the chemical reactions on the Ti surface during the anodization. In contrast, in acid solutions the coefficient of film thickness growth decreases with increasing acid concentrations, probably due to intense chemical dissolution of the film during its anodic formation.[12]

Electrolyte temperatures have only a small net effect on the coefficient of film thickness growth as seen in Table II. The effect is somewhat greater in more concentrated KOH solutions, *i.e.*, 5 M, than in 1 and 0.1 M.

The potential at which the anodic film is formed has the most profound effect on the film thickness growth and also determines the properties of the film produced. During formation of the films, at large anodic voltages, oxygen evolution takes place, indicating that efficiency of the film formation reaction is less than 100%. With oxygen evolution, titanium ion dissolution into the solution also takes place. This was analyzed by a colorimetric method using hydrogen peroxide. The dissolution of the oxide could either involve local attack, leading to the formation of pores (as seen at large voltages), or it could occur uniformly across the surface (as seen at low anodization voltages). Considering the fact that anodic Ti oxide formation is always accompanied by oxygen evolution, it would be reasonable to assume that inside the pores, the oxygen evolution reaction proceeds until the pore is filled with electrically insulating gas. The pores filled with electrically insulating gas represent a dielectric, or some kind of microcapacitor, which is short-circuited by the local breakdown. When the applied anodic voltage achieved some critical values (breakdown voltage), the local breakdown occurs, and the electric energy stored in the microcapacitor converts to thermal energy in the form of sparks and leads to fast dissolution of the film. This local destruction of anodic film makes a spontaneous local increase of conductivity, usually by many decades.

Ohtsuka *et al.*,[7] from surface observations of anodic surface films formed on Ti electrode in HCl, H_2SO_4, and H_3PO_4, reported that the breakdown commences at 5.5 V, producing a number of crater-like cracks which will provide leakage paths for ionic current. At potentials more positive than 7.5 V the ionic current concentrates at the cracks forming a thin oxide layer whose thickness becomes greater than that of the film formed at more negative potentials. These authors have shown a linear relationship between film thickness and applied potential only up to 7.5 V. The big discrepancy between ours and their results regarding the linear relationship between film thickness and applied voltage, probably comes from the difference in surface preparation of the Ti electrode. They utilized surfaces etched in a mixture of HNO_3 and HF. We suspect that etching in these solutions provokes fast dissolution of Ti substrate during the anodization. This is in contrast with previous results where the formed film on electropolished surfaces is much more resistant.[13,15]

The complex refractive indexes determined at low concentrations of KOH have similar values as those obtained in low concentrations of acid solutions.[6] The breakdown voltage decreases with increase in KOH concentration. Hence at large concentrations of KOH, the theoretical fitted curves are shorter and determination of refractive indexes are less precise. For example, in 5 M KOH, up to 6 V, 12 ellipsometric measurements were performed, each at a potential perturbation of 0.5 V. From these 12 experimental points it is possible to determine very precisely the coefficient of film thickness growth from the slope of the linear plot. However, the theoretical fitted curve would be very short and calculation of refractive indexes for this concentration is not recommended.

In all our calculations we suppose that the refractive indexes do not change with film thickness. This assumption is quite reasonable since the same values are obtained in Fig. 1 for the voltage difference between 0 and 56 V and on Fig. 2 for the voltage difference between 20.5 and 76.5 V. Changes of refractive indexes are observed only near and above the breakdown voltages.

Some authors claim that the anodic films on Ti surfaces are transparent and insulating, *i.e.*, the imaginary part of refractive indexes $k_2 = 0$.[24] Our ellispometric measurements have shown that the values of k_2 are near zero but are never zero, *i.e.*, the anodic films are not insulating but semiconducting. For the voltages close to and above the breakdown potential the value of k_2 increases as a result of increasing defects in the film. The defects present in the film also lead to increased conductivity. The values for the real part of the refractive indexes for 0.1 M KOH (see Table I) are in accordance with theoretical explanations in Ref. 18 where it is proved that for the same type of electrolyte, with increasing coefficient of film thickness growth the real part of refractive indexes decreases.

Our micro-Raman spectra generally confirmed the structure of anodic oxide films, formed on Ti surface at various applied voltages, as seen by other authors utilizing Raman spectroscopy techniques. The biggest discrepancy is in the anodic voltage limit indicating beginning of crystallization, *i.e.*, transformation of amorphous TiO_2 film to anatase form. This discrepancy results from differences in modes of surface preparation of Ti electrodes, concentration, and nature of the utilized electrolyte solutions and measurement techniques with Raman spectroscopy. The beginning of crystallization was at 7.5 V in HCl and H_3PO_4,[7] over 10 V in deaerated borate solution, pH 8.4,[26] 12 V in 1 M HNO_3, and 40 V in 1 M KOH.[27] Generally two sources of laser effects can shift the values of crystallization voltage, strong laser power initiating local crystallization in the area where the laser beam falls on the electrode surface and losses in intensity of the Raman scattered rays during *in situ* measurements. The intensity losses of *in situ* measurements with conventional Raman spectroscopy are estimated to be approximately 70% and are due to reflection and absorption of the incident and Raman scattered light from the electrochemical cell and electrolyte solution.[27] The advantage of micro-Raman *ex situ* measurements is collection and detection of Raman scattered lights only from the investigated surface, while the advantage of Raman *in situ* measurements is collection and detection of Raman scattered light during the potential control of the electrode surface and elimination of all possible effects due to side reactions of the electrode surface films with atmosphere after anodization interruption.

The shape of our micro-Raman spectra for well-crystallized anatase form is almost identical with anatase spectra reported in literature.[27-29] Only a small difference in intensities and shift in the wavenumbers of some bands is noticeable. These differences are a little bit bigger for the mixture of four mineral forms (anatase, brookite, rutile, and corundum) seen for an anodization time of 10 s in 1 M KOH at 72 V (Fig. 6). This could probably be due to the difference in time of anodization. The composition ratio of the mixture changes every second of anodization; thus, for anodization time of 30 s predominately rutile structure and after 60 s only rutile structure was detected (Fig. 7).

From a systematic study of micro-Raman spectra it can be concluded that anatase is the only crystalline form of TiO_2 formed during the anodization. Brookite and corundum mineral form are intermediate products during the local heating of the Ti surface by short anodic spark. The rutile mineral form can be obtained only by thermal oxidation[17] or by heating due to the existence of a spark for a long time during anodization.

Conclusions

Ellipsometry and micro-Raman spectroscopy were used to study the oxide films formed on Ti in strong alkaline KOH solutions at

different anodic potentials. At all concentrations of KOH studied, the thickness of the oxide films increases linearly with applied voltage. At room temperature the rates of film thickness growth with applied voltage as determined ellipsometrically are 2.38, 2.49, and 3.47 nm V^{-1} in 0.1, 1, and 5 M KOH, respectively. The complex refractive indexes at a wavelength of 546.1 nm are found to be: $\hat{n}_2 = 2.24(1\text{-}0.006.i)$ and $\hat{n}_2 = 2.39(1\text{-}0.009.i)$ for anodic oxide films formed in 0.1 and 1 M KOH, respectively. In 5 M KOH the theoretical fitted curve using the Fresnel equation to experimentally measured Δ-ψ is shorter as a result of the film breakdown at a potential of 6 V and determination of $\hat{n}_2$ is less precise. The crystallization of amorphous anodic films, determined by micro-Raman spectroscopy strongly depends on the concentrations of KOH solutions, applied voltages, and times of anodization. In 0.1 M KOH the transformation of amorphous TiO_2 to anatase structure begins at 25 V, while in 1 M KOH it begins at 15 V. In 1 M KOH at an applied anodic voltage of 72 V visible sparks appear on the electrode surface and transformation of the anatase to rutile form begins. During this transformation brookite and corundum structures form as the intermediate products. The final structure is TiO_2 rutile formed as a result of heating the Ti surface due to sparks formed during the anodization process.

The University of South Carolina assisted in meeting the publication costs of this article.

References

1. Lj. Arsov, *J. Eng. Phys.*, **1979**, 5.
2. F. Di Quarto, K. Doblhofer, and H. Gerischer, *Electrochim. Acta*, **23**, 195 (1978).
3. J. L. Ord, D. J. DeSmet, and J. Beckstead, *J. Electrochem. Soc.*, **136**, 2178 (1989).
4. F. Climent and R. Capelades, *Electrochim. Acta*, **33**, 433 (1988).
5. K. Fushimi, T. Okawa, K. Azumu, and M. Seo, *J. Electrochem. Soc.*, **147**, 524 (2000).
6. A. Efremova and Lj. Arsov, *Electrochim. Acta*, **37**, 2099 (1992).
7. T. Ohtsuka, M. Masuda, and N. Sato, *J. Electrochem. Soc.*, **132**, 787 (1985).
8. G. Blondeau, M. Froelicher, M. Froment, and A. Hugot Le-Goff, *J. Less-Common Met.*, **56**, 215 (1997).
9. I. Sangli and S. Visvanathan, *Electrochim. Acta*, **7**, 575 (1962).
10. A. Prusi and Lj. Arsov, *Corros. Sci.*, **33**, 153 (1992).
11. F. Faizulin and D. Baitalov, *Zasch. Metallov*, **4**, 11 (1968).
12. Lj. Arsov, M. Froelicher, M. Froment, and A. Hugot Le-Goff, *J. Chim. Phys.*, **3**, 275 (1975).
13. Lj. Arsov, *Electrochim. Acta*, **30**, 1645 (1985).
14. M. Pourbaix, *Atlas d'equilibres electrochim.*, Gauthier Villars, Paris (1963).
15. Lj. Arsov, *Electrochim. Acta*, **6**, 663 (1982).
16. B. Johnson and R. W. Christy, *Phys. Rev. B*, **9**, 5056 (1974).
17. A. Hristova, Lj. Arsov, B. N. Popov, and R. E. White, *J. Electrochem. Soc.*, **144**, 2318 (1997).
18. A. Efremova and Lj. Arsov, *J. Phys. (France)*, **2**, 1353 (1992).
19. A. Hugot Le-Goff, *Thin Solid Films*, **142**, 193 (1986).
20. J. R. Birch and T. D. Burleigh, *Corrosion (Houston)*, **56**, 1233 (2000).
21. Lj. Arsov, C. Kormann, and W. Plieth, *J. Raman Spectrosc.*, **22**, 573 (1991).
22. S. H. Shin, R. L. Aggarwal, and B. Lax, *Phys. Rev. B*, **9**, 583 (1974).
23. R. Menard, *J. Opt. Soc. Am.*, **52**, 427 (1962).
24. C. K. Dyer and J. S. Leach, *Electrochim. Acta*, **23**, 1387 (1978).
25. G. Blondeau, M. Froelicher, M. Froment, and A. Hugot Le-Goff, *Thin Solid Films*, **42**, 147 (1977).
26. T. Ohtsuka, J. Guo, and N. Sato, *J. Electrochem. Soc.*, **133**, 2473 (1986).
27. Lj. Arsov, C. Kormann, and W. Plieth, *J. Electrochem. Soc.*, **144**, 2318 (1997).
28. U. Balachandran and N. G. Eror, *J. Solid State Chem.*, **42**, 276 (1982).
29. T. Ohsaka, F. Izumi, and Y. Fujiki, *J. Raman Spectrosc.*, **7**, 321 (1978).